

## The Behavior of Nanometer-Sized Ga as Observed by PAC

St. Lauer, H. Ehrhardt, H.G. Zimmer, H. Wolf, and Th. Wichert  
*Technische Physik, Universität des Saarlandes, D-66041 Saarbrücken, Germany*

**Keywords** : PAC, Tungsten, Gallium, Nanocomposites, Thin films

### Abstract

The local structure of nanometer-sized Ga was investigated in the nanocomposite WGa as well as in thin Ga films and in Ga, covering the surface of nanometer-sized W powder. The perturbed  $\gamma\gamma$  angular correlation spectroscopy was used, which supplies information about the local lattice surroundings of the radioactive probe atom  $^{111}\text{In}$ . In the nanocomposite WGa two local structures were detected via their characteristic electric field gradients. Also the different Ga films and the Ga-W mixture exhibited clear deviations from the bulk behavior.

### Introduction

Nanocrystalline materials offer a wide field of new applications due to their properties, which differ from and often are superior to those of polycrystals or single crystals. One promising property is the ability of forming compounds, the components of which are immiscible under normal conditions, such as W and Ga. In order to study the formation of nanocrystalline compounds along with their properties, like structure and stability, on an atomic scale, locally sensitive experimental techniques are needed. In this paper, perturbed  $\gamma\gamma$  angular correlation spectroscopy (PAC) is used as the microscopic tool for the investigation of the nanocrystalline compounds.

The paper starts with the results obtained from the nanocomposite WGa, which was prepared by inert gas condensation. The introduced radioactive  $^{111}\text{In}$  atoms, serving as probe atoms for the PAC experiments, yield information about their direct environment by measuring electric field gradients (EFG). For the interpretation of the observed local structures, additional samples, consisting of differently prepared W-Ga compounds, were investigated, such as W/Ga multilayers, mixtures of W powder and liquid Ga, and W-Ga prepared by ball milling.

### Experimental details

The PAC experiments use the radioactive probe atom  $^{111}\text{In}$ , which decays to an excited state of its daughter isotope  $^{111}\text{Cd}$  (fig. 1). From this level two  $\gamma$  quanta are emitted, thereby populating a spin  $I = 5/2$  nuclear level with a lifetime of 123 ns. The emission probability of the second  $\gamma$  quantum with respect to the first one has a spatial anisotropy due to the conservation of angular momentum during the decay process. The nuclear quadrupole moment  $Q$  of the  $I = 5/2$  level is used for detecting the parameter of interest, namely the electric field gradient (EFG). The EFG is a second rank, traceless tensor, which in its principle axis system is completely described by two quantities: Its largest component  $V_{zz}$  and the asymmetry parameter  $\eta = (V_{xx} - V_{yy})/V_{zz}$ , for which the relation  $0 \leq \eta \leq 1$  holds, if  $|V_{xx}| \leq |V_{yy}| \leq |V_{zz}|$  is chosen. The hyperfine interaction of the quadrupole moment  $Q$  with the EFG at the site of the probe nucleus causes a threefold splitting of the  $I = 5/2$  level, or in a classical picture, a periodic motion of the nuclear spin, which leads to a modulation in time of the spatially anisotropic emission probability of the second  $\gamma$  quantum. This modulation is governed by the three frequencies  $\omega_1$ ,  $\omega_2$ , and  $\omega_3 = \omega_1 + \omega_2$ , resulting from the three possible energy differences of the split nuclear  $I = 5/2$  state (fig. 1). The frequencies are proportional to the product  $QV_{zz}$  and the strength of the EFG is usually expressed by the quadrupole coupling constant  $\nu_Q = eQV_{zz}/h$ , which is proportional to  $\omega_1$ . The value of the asymmetry parameter  $\eta$  is deduced from the ratio  $\omega_2/\omega_1$ . In a PAC experiment, the time between the first and the second  $\gamma$  quantum is recorded by  $\gamma$  detectors, which are arranged under fixed angles  $\theta$ . In case of

polycrystalline samples, the number of recorded coincidences, can be described in a good approximation by the function

$$N(\theta, t) = N_0 \cdot e^{-t/\tau} \cdot (1 + P_2(\cos\theta) \cdot R(t)) + B$$

with

$$R(t) = A_2 \cdot \left\{ f \cdot \left( s_0 + \sum_{n=1}^3 s_n \cos \omega_n t \right) + (1 - f) \right\}$$

After subtraction of the background B, the function of interest R(t) is obtained by combining the coincidence spectra N(θ,t) that were recorded for appropriate angles θ. P<sub>2</sub>(cos θ) is the Legendre polynomial. From the R(t) time spectrum the EFG parameters are extracted via the three frequencies ω<sub>1</sub>, ω<sub>2</sub>, and ω<sub>3</sub>. The amplitude of the modulation contains the information on the parameter f, the fraction of probe atoms, which resides in an environment that produces a particular non-zero EFG; (1-f) denotes the fraction of probe atoms with zero EFG. In the case of different environments characterized by non-zero EFG, f has to be split into different fractions f(i), whereby each is represented by its own characteristic frequency triplet ω<sub>n</sub>(i). A more detailed description of PAC spectroscopy can be found elsewhere [1]. The values for v<sub>Q</sub> and η, which are presented in this paper, were measured at 77 K.

The WGa samples were prepared by inert gas condensation [2,3], whereby W was sputtered by Ar<sup>+</sup> ions and, simultaneously, Ga was thermally evaporated into an Ar atmosphere. After condensation, the nanometer-sized W crystallites (≈10 nm), which were covered by Ga layers, were deposited on a cold-finger. Subsequently, the material was compacted into pellets of about 8 mm diameter and 0.5 mm thickness. The WGa pellets, which are subject of these investigations, had Ga contents of 50 at% and 33 at%. In all cases, the <sup>111</sup>In probe atoms were diffused into the different samples *ex-situ*, i.e. following the preparation of the sample, under vacuum at T = 700 K for several hours.

Layers of Ga on glass and W/Ga multilayers were produced by evaporation of the components under high vacuum conditions onto a substrate at room temperature. The thickness was controlled by a quartz monitor.

Additional investigations were performed at a WGa composite produced by mixing nanometer-sized W powder and liquid Ga. This mixture was heated at 700 K along with the <sup>111</sup>In probes under vacuum for one hour. The nanometer-sized W powder used was prepared by ball milling of a W foil for 100 h. Another sample was composed by ball milling of a mixture of W powder and Ga for 2 h and subsequent diffusion with <sup>111</sup>In.

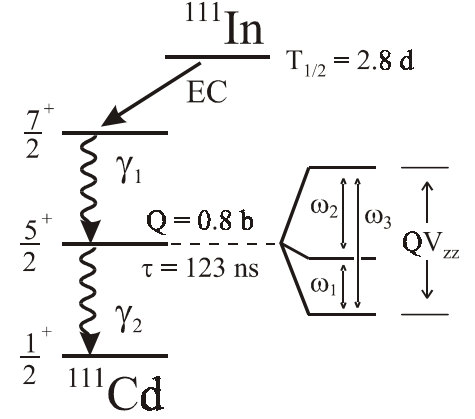


**Fig. 1** : Decay scheme of the PAC probe <sup>111</sup>In.

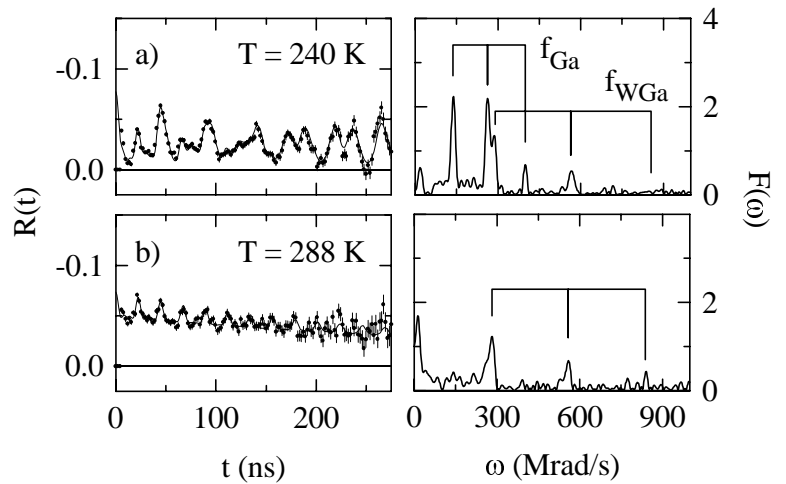


**Fig. 2** : PAC spectra of a WGa (50 at% Ga) sample diffused with <sup>111</sup>In and measured at different temperatures.

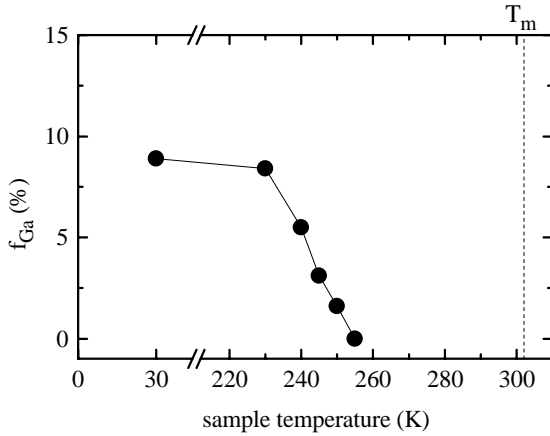


**Fig. 3** : The fraction  $f_{Ga}$  of  $^{111}\text{In}$  atoms ( $\nu_Q = 147$  MHz,  $\eta = 0.2$ ) as a function of sample temperature in the composite WGa (33 at% Ga).

atoms in the environment of the probe atoms fluctuate so rapidly that the resulting EFG average to zero. A more detailed investigation of the melting-transition for a sample with a Ga content of 33 at% is shown in fig. 3. The fraction of  $^{111}\text{In}$  atoms that is exposed to the EFG of 147 MHz decreases at sample temperatures around 240 K. That means, the melting-point of  $\alpha$ -Ga is depressed from 302 K to 240 K. In addition, there is no sharp melting-transition visible, but the whole process occurs over a temperature range of about 20 K. Since it is known that the melting-temperature depends on the size of crystallites [5], the depression of the melting-point of  $\alpha$ -Ga is attributed to the small particle size and the smeared out melting-transition is explained by a size distribution of the Ga crystallites. It is important to note that the PAC results describe the WGa composite after an additional temperature treatment at 700 K, needed for the diffusion of  $^{111}\text{In}$ . Directly after preparation, the WGa material showed neither crystalline Ga nor a melting-transition, as was concluded from differential scanning calorimetry (DSC). Tempering the sample leads to a growth of W crystallites, as could be shown by X-ray diffraction (XRD), and to the formation of  $\alpha$ -Ga precipitates (PAC).

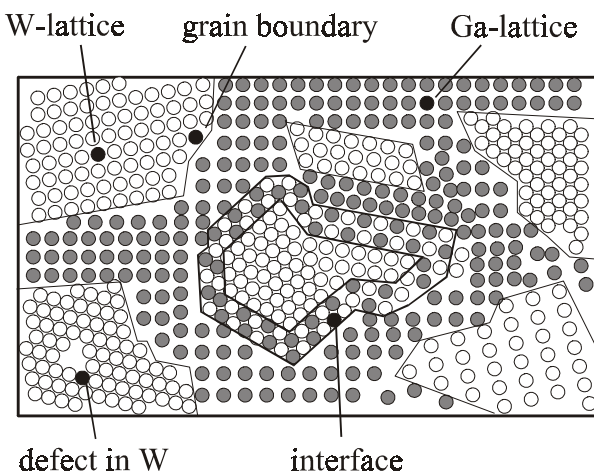


**Fig. 4** : Microscopic model for the composite WGa, consisting of W (open circles) and Ga atoms (grey circles). Possible sites for the incorporation of  $^{111}\text{In}$  (black circles) are indicated.

## Results and discussion

### Nanocomposite WGa

The PAC spectrum of a WGa sample (50 at% Ga), prepared by inert gas condensation and diffused with  $^{111}\text{In}$ , is shown in fig. 2. At temperatures  $T \leq 240$  K, two EFG are observed, as is visible by their respective frequency triplets. The first EFG, the fraction of which is denoted by  $f_{Ga}$ , is characterized by  $\nu_Q = 147$  MHz and  $\eta = 0.2$ . Since this EFG is well-known for  $^{111}\text{In}$  residing in the orthorhombic lattice of  $\alpha$ -Ga [4], it is concluded that 25 % of the  $^{111}\text{In}$  atoms are incorporated in a crystalline  $\alpha$ -Ga phase as part of the composite WGa.

The signal due to  $\alpha$ -Ga vanishes in the PAC spectrum measured at 288 K (fig. 2b), because of the melting of the Ga crystals. In liquid Ga, the atoms in the environment of the probe atoms fluctuate so rapidly that the resulting EFG average to zero. The second EFG, with  $\nu_Q = 320$  MHz (fig. 2), is axially symmetric and is neither known for pure W nor for pure Ga. This EFG, the fraction of which is denoted by  $f_{WGa}$ , is obviously typical for WGa and is visible up to at least 500 K. The axial symmetry of the EFG hints to a tetragonal or hexagonal local symmetry of the corresponding atomic arrangement about the  $^{111}\text{In}$  probe atoms. A schematic model of the composite WGa, based on the PAC results, is presented in fig. 4. It consists of nanocrystalline W crystallites, which are embedded in a Ga matrix. The Ga covers the W particles and, additionally, forms orthorhombic Ga crystallites, as is evident from the fraction  $f_{Ga}$  of  $^{111}\text{In}$  atoms. Besides the Ga lattice, in fig. 4 other possible sites for the  $^{111}\text{In}$  atoms are indicated that might effect the 320 MHz EFG. From experiments at nanocrystalline W [6], it is concluded that a

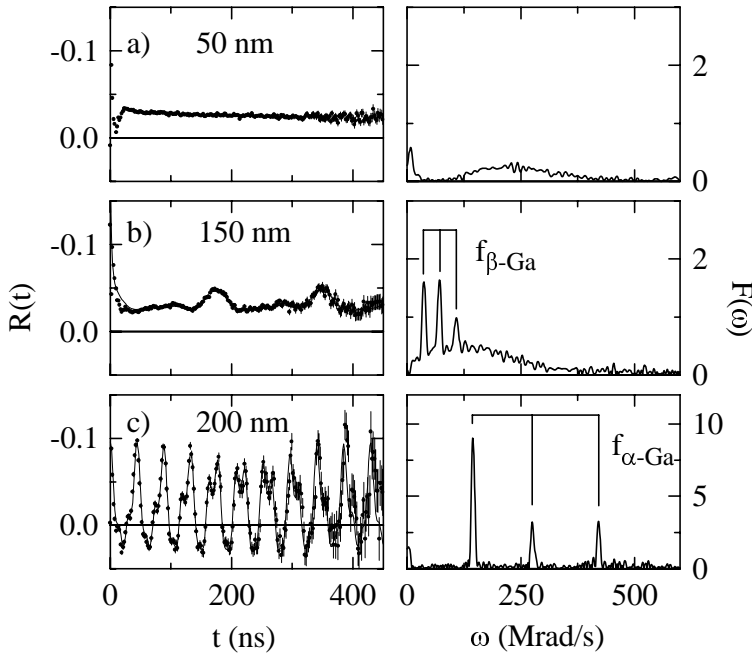


**Fig. 5** : PAC spectra of  $^{111}\text{In}$  doped Ga films of different thicknesses evaporated on glass.

were deposited on a glass substrate, in order to prepare large interface regions. The spectrum of a 50 nm thick Ga film (fig. 5a) shows a frequency distribution, which is centred at 250 MHz, and, therefore, indicates no crystalline structure. In a film with a thickness of 150 nm (fig. 5b), 15 % of the  $^{111}\text{In}$  atoms are exposed to a well-defined EFG, characterized by  $\nu_Q = 38$  MHz and  $\eta = 0.15$ . The corresponding XRD pattern (fig. 6) identifies this structure as monoclinic  $\beta$ -Ga. The EFG parameters for  $\beta$ -Ga obtained here differ from those given by Heubes and co-workers [7]. Due to the different experimental conditions and the spectrum presented in [7], it is difficult to settle the discrepancy at this time. In a Ga layer with a thickness of 200 nm (fig. 5c), about 75 % of the  $^{111}\text{In}$  probes are part of orthorhombic  $\alpha$ -Ga, as indicated by the characteristic EFG of 147 MHz. This layer exhibits no depression of the melting-temperature, in contrast to the results obtained in case of the composite WGa (see fig. 3). Analogous experiments at W/Ga multilayers yield comparable results. This observation could be explained by the fact that the number of interface sites is too small to be observable because of the relative large thicknesses of the used Ga films of 150 nm and 200 nm.

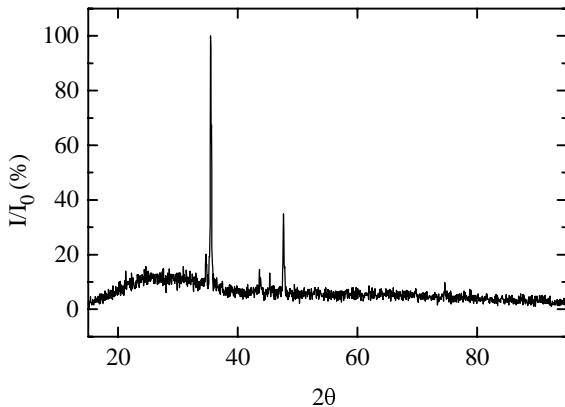


**Fig. 6** : XRD pattern of the 150 nm thick Ga film on glass, measured at 77 K (compare fig. 5b).

diffusion of In into the W crystallites at such low temperatures as 700 K does not seem to be probable. Also an occupation of grain boundary sites is not likely because it would not result in a sharp EFG, but rather in a broad frequency distribution. Thus, a possible structure giving rise to the fraction  $f_{\text{WGa}}$  might consist of an ordered arrangement of W and Ga atoms at the interface between both constituents.

#### Ga layers

In order to get more information about the origin of the EFG, characterized by  $\nu_Q = 320$  MHz, additional experiments at the W-Ga system were performed. In a first step, thin Ga layers of various thicknesses

#### WGa mixture

At a WGa composite, which was produced by mixing W powder with liquid Ga and followed by a heat treatment at 700 K for the diffusion of  $^{111}\text{In}$ , the recorded PAC spectrum is governed by two EFG (fig. 7): The well-known EFG for  $\alpha$ -Ga ( $\nu_Q = 147$  MHz,  $\eta = 0.2$ ) and a second new EFG, characterized by  $\nu_Q = 23$  MHz and  $\eta = 0.15$ . About  $f_{\text{Ga}} = 25$  % of the  $^{111}\text{In}$  atoms are part of the first environment, about  $f_{\gamma\text{-Ga}} = 60$  % are part of the second one. At a temperature of 290 K the EFG with  $\nu_Q = 23$  MHz disappears (fig. 7b), what is typical for a the melting-

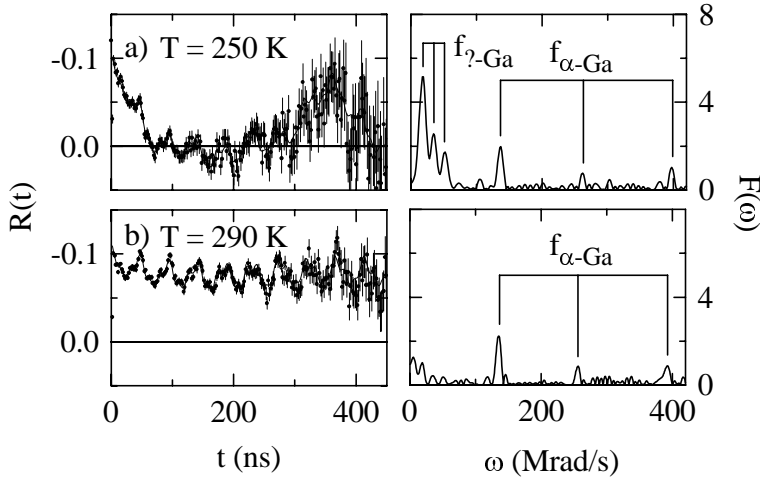


**Fig. 7 :** PAC spectra of the  $^{111}\text{In}$  doped mixture of W powder and Ga measured at different temperatures  $T$ .

observation and the melting-transition near room temperature favour the interpretation that this EFG is caused by the non-cubic lattice of a new Ga-phase, with a lattice structure, which could not be identified, up to now. This association of the EFG with Ga is supported by the observation of an EFG in Ga metal, characterized by  $\nu_Q = 23$  MHz, by H. Haas and D.A. Shirley [9]. But, the authors did not publish an analysis of the corresponding crystalline structure.

If the mixture, consisting of W powder and Ga, was milled for 2 h and, subsequently, diffused with  $^{111}\text{In}$ , the PAC spectrum showed no indications of crystalline Ga. Neither a well-defined EFG, nor an indication of fluctuating Ga atoms was observed, when the sample temperature was increased from 77 K to 295 K. An EDX analysis, however, yielded a Ga content of about 50 %. Obviously, ball milling effected a completely different local structure of the Ga atoms in this case, as compared to the unmilled material, which contained two crystalline Ga phases ( $\alpha$ -Ga and  $\gamma$ -Ga).

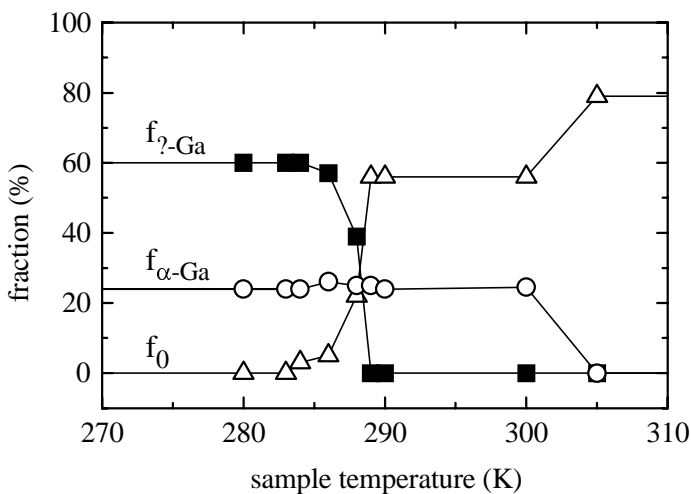


**Fig. 8 :** The fraction of the two Ga phases in the W-Ga mixture (see fig. 7) as a function of temperature. Here,  $f_0$  denotes  $^{111}\text{In}$  atoms exposed to an EFG equal to zero.

transition. The melting behaviour of these two Ga phases, being part of the prepared WGa mixture, is shown in fig. 8. The fraction  $f_{\gamma\text{-Ga}}$  goes to zero above 287(2) K and the fraction  $f_{\alpha\text{-Ga}}$  at the bulk value of  $\alpha$ -Ga at 302 K. In both cases, the fractions of  $^{111}\text{In}$  atoms in the respective molten phase  $f_0$  were exposed to a zero EFG.

The temperature dependence of the coupling constant of the EFG, characterizing the new phase (23 MHz), follows the relation  $\nu_Q(T) = \nu_Q(0) \cdot (1 - B \cdot T^{3/2})$ , which is typical for lattice field gradients in non-cubic metals [8]. This

## Summary

The different systems, which were examined by PAC, are listed in tab. 1. In the nanocomposite WGa, prepared by inert gas condensation, two crystalline structures were detected: The formation of orthorhombic Ga precipitates, correlated with the growth of W crystallites during the temperature treatment needed for the  $^{111}\text{In}$  diffusion. This Ga phase, designated as  $\alpha'$ -Ga in tab. 1, is characterized by the same EFG as conventional bulk Ga, but exhibits a depression of the melting-temperature from 302 K to 240 K. The origin of the second crystalline structure, characterized by  $\nu_Q = 320$  MHz and  $\eta = 0$ , is not yet understood, but an ordered arrangement of W and Ga atoms at the interface between both components seems to be probable. Other W-Ga compounds could

not reproduce this structure, but showed the formation of different Ga phases. The PAC results at Ga films on glass or W yielded a non-crystalline structure, crystalline  $\beta$ -Ga, or crystalline  $\alpha$ -Ga, depending on the thickness of the Ga layer. At a mixture composed of W and Ga, a new EFG, probably belonging to a new Ga phase with a melting-temperature of 287 K, was detected. Finally, ball milling of the same material resulted in a completely non-crystalline Ga structure.

**Table 1** : EFG characterizing the different Ga environments.

	$\alpha$ -Ga	$\alpha'$ -Ga	"WGa"	$\beta$ -Ga	?-Ga
$\nu_Q$	147 MHz	147 MHz	320 MHz	37 MHz	23 MHz
$\eta$	0.2	0.2	0.0	0.15	0.15
$T_m$	302 K	$\approx$ 240 K	> 500 K	< 290 K	287 K
occurrence	bulk & Ga film ( $\geq$ 200 nm)	nanocomposite WGa	nanocomposite WGa	Ga film (100-150 nm)	mixture of nanocrystalline W and Ga

In future experiments, it is planned to incorporate the  $^{111}\text{In}$  probe atoms *in-situ* during the inert gas condensation process to avoid the additional heat treatment of the diffusion process. The experiments at the W/Ga multilayers will be refined with respect to smaller thicknesses of the Ga layers in order to increase the relative fraction of interface sites. Finally, different parameters for the ball milling process, e.g. the milling time, might result in structures, which differ from those presented here.

### Acknowledgements

The authors would like to thank Dr. W. Krauss for the preparation of the composite WGa and for fruitful discussions. We thank Dr. J. Albers and Mr. P. Huber for the XRD investigation and Dr. D. Wilhelm for the EDX analysis. The financial support by the DFG as part of the SFB 277 is thankfully acknowledged.

### References

- 1.) Th. Wichert and E. Recknagel, in "Microscopic Methods in Metals", ed. U. Gonser, Topics in Current Physics **40**, 317 (1986)
- 2.) H. Gleiter, J. Appl. Cryst. **24**, 79 (1991)
- 3.) R.W. Siegel, in "Processing of Metals and Alloys", eds. R.W. Cahn, P. Haasen, E.J. Kramer, Materials Science and Technology **15**, 583 (1991)
- 4.) W. Keppner, U. Körner, P. Heubes, and G. Schatz, Hyp. Int. **9**, 293 (1981)
- 5.) F.G. Shi, J. Mater. Res. **9**, 1307 (1994)
- 6.) H. Wolf, H.G. Zimmer, T. Filz, and Th. Wichert, Nanostructured Materials **6**, 613 (1995)
- 7.) P. Heubes, D. Korn, G. Schatz, and G. Zibold, Phys. Lett. **74A**, 267 (1979)
- 8.) J. Christiansen, P. Heubes, R. Keitel, W. Klinger, W. Loeffler, W. Sandner, and W. Witthuhn, Z. Physik **B24**, 177 (1976)
- 9.) H. Haas and D.A. Shirley, J. Chem. Phys. **58**, 3339 (1973)